https://doi.org/10.5194/egusphere-2026-6962
Preprint. Discussion started: 20 November 2026
© Author(s) 2026. CC BY 4.0 License.

Compensating biases in CMIP6 TOA radiative-flux trends and their implications for EEI-based constraints on equilibrium climate sensitivity

Takuro Michibata[1] and Momoka Nakanishi[1,2]

[1]Research Institute for Applied Mechanics, Kyushu University, Fukuoka 816-8580, Japan
[2]Interdisciplinary Graduate School of Engineering Sciences, Kyushu University, Fukuoka 816-8580, Japan

Correspondence: Takuro Michibata (michibata@riam.kyushu-u.ac.jp)

Abstract. Earth's energy imbalance (EEI) is a key metric for monitoring climate. Decomposing the all-sky net EEI trend into shortwave (SW) and longwave (LW) components and separating clear-sky and cloud radiative effect (CRE) contributions provide insights into factors contributing to radiative forcing and feedbacks. Herein, we quantify trends in nine TOA radiative-flux components using CERES satellite data and 34 CMIP6 models. Decomposed radiative-flux trends, particularly under clear-sky conditions, are useful for constraining equilibrium climate sensitivity (ECS), implying a moderate ECS range of 2.0–4.5 K. However, biases in clear-sky and CRE trends compensate for each other, yielding an apparently consistent net EEI trend relative to CERES. These compensating biases may complicate the physical interpretation of EEI-based constraints on ECS. To understand the mechanisms underlying these biases, the combined use of cloud cover trends provides a useful approach. Cloud cover and EEI trends covary, and some CMIP6 models even misrepresent the sign relative to the negative trend observed. Robust constraints therefore require consistency between the net EEI trend and its SW, LW, clear-sky, and CRE components, and cloud cover trends provide an additional physical diagnostic. Temporal variations in CERES radiative-flux trends likely reflect a combination of time-dependent radiative forcing, feedback responses, and internal variability. Therefore, the inferred ECS range should be interpreted as indicative rather than definitive. Our findings highlight the importance of evaluating component-level agreement and sensitivity to the analysis period.

1 Introduction

An accurate understanding of climate responses to perturbed radiative forcing is fundamental to the climate science community (Forster et al., 2021). One of the largest uncertainties lies in feedback processes, particularly those associated with clouds. Cloud responses to global warming are highly complex, involving changes in their macrostructures (e.g., cloud amount and altitude) and microstructure (e.g., cloud phase and effective radius), thereby contributing to both shortwave (SW) feedback (McCoy et al., 2020; Lutsko et al., 2022) and longwave (LW) feedback (Tan and Storelvmo, 2019; Nakanishi and Michibata, 2025), which directly cause uncertainties in equilibrium climate sensitivity (ECS) (Sherwood et al., 2020; Meehl et al., 2020; Cesana et al., 2024). Notably, recent reductions in aerosol emissions affect the radiation budget through both aerosol–radiation and aerosol–cloud interactions (Hodnebrog et al., 2024; Samset et al., 2025), while changes in surface albedo and water vapor

https://doi.org/10.5194/egusphere-2026-6962
Preprint. Discussion started: 20 November 2026
© Author(s) 2026. CC BY 4.0 License.

represent additional non-cloud contributions (Taylor et al., 2007), thereby complicating the attribution of observed radiative trends and their implications for climate predictions (Michibata et al., 2025).

Earth's energy imbalance (EEI), defined as the difference between the energy entering Earth's system and that leaving for space (Hansen et al., 2011; Trenberth et al., 2014), is widely used as a headline metric for "planetary health" (Raghuraman et al., 2021; Forster et al., 2024; Allan and Merchant, 2025). EEI represents the total effective radiative forcing (ERF) minus the radiative feedback in response to surface temperature change, indicating how much forcing still translates into heat uptake (Skeie et al., 2024). The Clouds and the Earth's Radiant Energy System (CERES) instrument has observed the Earth's energy budget since March 2000, consistent with *in situ* measurements (Von Schuckmann et al., 2023; Hakuba et al., 2024; Cheng et al., 2024), enabling the derivation of robust EEI trends over more than two decades (Loeb et al., 2024, 2025; Mauritsen et al., 2025).

Motivated by long-term satellite records, several modeling studies have attempted to reproduce satellite-inferred EEI trends using global climate models (GCMs). A multimodel ensemble using five GCMs reproduced the observed EEI trend but showed a 10–40% underestimation owing to biases in both SW and LW (Hodnebrog et al., 2024). This finding is consistent with other GCM ensembles (Schmidt et al., 2023), and can be further linked to biases in clear-sky and cloud radiative effect (CRE) trends (Stephens et al., 2022). Because the recent acceleration in global warming is associated with decreasing aerosol emissions (Gettelman et al., 2024; Hodnebrog et al., 2024; Samset et al., 2025), an accurate representation of temperature evolution requires an all-sky EEI consistent with both clear-sky fluxes (i.e., sensitivity to aerosols, greenhouse gases, vapor, and surface albedo) and CRE. However, few studies have explored detailed EEI trend decomposition using a large ensemble of state-of-the-art GCMs (Myhre et al., 2025), and little agreement exists on how EEI trends constrain future warming (Michibata et al., 2025).

To this end, we quantify TOA radiative-flux trends for nine scenes representing all-sky, clear-sky, and CRE contributions for the net, SW, and LW components. Using 24 years of CERES satellite retrievals and 34 CMIP6 models, we discuss their applicability to constraining ECS. We also show that compensating errors between clear-sky and CRE trends exist in the CMIP6 models, producing an apparently consistent all-sky net EEI trend. This suggests that although the EEI trend can constrain ECS, such compensation complicates the physical interpretation and robustness of the constraint.

2 Materials and Methods

2.1 CERES satellite product

The CERES EBAF Edition 4.2.1 monthly averaged $1^\circ \times 1^\circ$ gridded product (Kato et al., 2018; Loeb et al., 2018; Doelling, 2026) was used in this study. This product includes SW, LW, and net radiative fluxes for the TOA and the surface, and we used 24 years of data from January 2001 to December 2024. The trends estimated from CERES have been reported to be robust for the Aqua/Terra platform comparison (Loeb et al., 2022), and are consistent with *in situ* measurements (Loeb et al., 2021a) within 0.1 $\mathrm{W\,m^{-2}\,dec^{-1}}$. For clear-sky radiative fluxes, we used the clear-sky over the total area definition (*clr_t*) rather than the clear-sky over cloud-free pixels only definition (*clr_c*) to ensure consistency with how the models compute clear-sky fluxes

https://doi.org/10.5194/egusphere-2026-6962
Preprint. Discussion started: 20 November 2026
© Author(s) 2026. CC BY 4.0 License.

(Hodnebrog et al., 2024). Cloud coverage and cloud optical depth based on Terra/Aqua MODIS retrievals (Trepte et al., 2019) are also available in the product.

2.2 CMIP6 climate models

We used 34 CMIP6 climate models that satisfied available outputs to compute EEI (*rsdt, rsut, rlut, rsutcs, rlutcs*) and cloud cover (*clt*) trends. The models and ensemble information used in this study are listed in Table S1 along with ECS values (Zelinka et al., 2020; Forster et al., 2021; Michibata et al., 2025). Summary statistics of the trends are provided in Table S2. The CMIP6 models were analyzed for the period January 2001 to December 2014, corresponding to the overlap between the historical simulation record and CERES satellite. For consistency between observations and models, the analysis period was matched, and scenario runs after 2015 were excluded to avoid introducing scenario-dependent forcing differences.

2.3 Statistics

Linear trends were estimated for both the observations and the models. To reduce seasonality, monthly outputs were aggregated into annual means before estimation, and the resulting trends closely matched those obtained from the original monthly series. Statistical significance was evaluated using a two-tailed Student's *t*-test at the 95% confidence level. For global mean values, the 95% confidence intervals were computed using *t*-based critical values and standard errors estimated from the residuals of the linear trend model.

3 Results

3.1 Decomposing radiative-flux trends for different components

The CERES satellite-retrieved all-sky net EEI trend is decomposed into clear-sky and CRE contributions for the SW and LW components (Figure 1). For the global mean, the all-sky net EEI trend of +0.45 $\mathrm{W\,m^{-2}\,dec^{-1}}$ during 2001-2024 is dominated by a positive SW trend of +0.83 $\mathrm{W\,m^{-2}\,dec^{-1}}$, which is partially offset by a negative LW trend of -0.39 $\mathrm{W\,m^{-2}\,dec^{-1}}$ (Figure 1a–c). Geographical distributions include both positive and negative values, and show a complex pattern. However, all-sky trends are statistically significant over the northern midlatitudes (30°N–50°N) across all radiation components, including net, SW, and LW (Figure S1).

This coherent positive EEI trend over the northern midlatitudes is found mainly in the clear-sky SW components (Figure 1d). The positive trends over East Asia, North America, and Europe are spatially consistent with the radiative response to reductions in anthropogenic aerosol emissions reported in recent studies (Loeb et al., 2021b; Hodnebrog et al., 2024; Samset et al., 2025).

A strongly positive clear-sky SW trend is also observed over the Arctic region. This trend is consistent with the surface-albedo response to sea-ice loss, which reduces reflected SW radiation and increases SW absorption. In contrast, the negative clear-sky LW EEI trend over the Arctic (Figure 1e) primarily reflects the temperature-mediated radiative response to strong

https://doi.org/10.5194/egusphere-2026-6962
Preprint. Discussion started: 20 November 2026
© Author(s) 2026. CC BY 4.0 License.

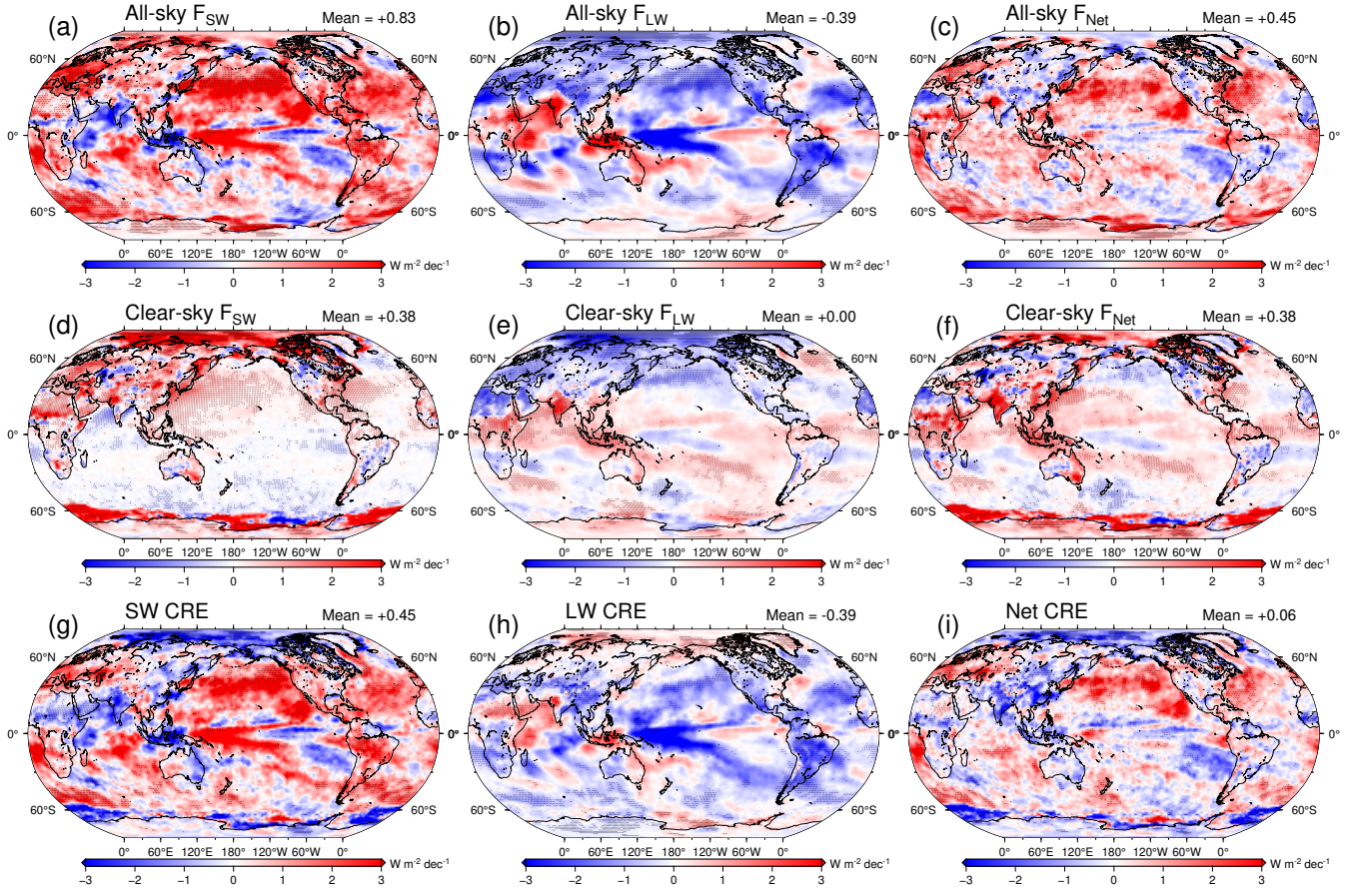


Figure 1. Geographical distributions of CERES satellite-retrieved TOA radiative-flux trends. Trends for (**a**) all-sky SW, (**b**) all-sky LW, (**c**) all-sky net, (**d**) clear-sky SW, (**e**) clear-sky LW, (**f**) clear-sky net, (**g**) SW CRE, (**h**) LW CRE, and (**i**) net CRE for the period January 2001–December 2024. Global mean values are provided at the top right of each panel. Dots indicate regions where trends differ significantly from zero at the 95% confidence level. Units are $\mathrm{W\,m^{-2}\,dec^{-1}}$, positive downward.

Arctic warming, dominated by the Planck response, with possible additional contributions from lapse-rate and water-vapor changes.

Over the tropics and subtropics, the positive clear-sky LW EEI trend is consistent with an increase in atmospheric water vapor, which reduces outgoing LW. This water-vapor radiative effect appears to offset the opposing temperature-mediated
90 Planck response in these regions (Loeb et al., 2021a). The spatial compensation between the negative Arctic and positive low-to-mid latitude LW trends results in a near-zero global-mean clear-sky LW EEI trend (Figure 1e). Although these yield a +0.38 $\mathrm{W\,m^{-2}\,dec^{-1}}$ clear-sky net EEI trend (Figure 1f), which almost matches the all-sky net EEI trend (Figure 1c), the geographical distribution of the all-sky EEI trend depends strongly on that of the CRE trend.

https://doi.org/10.5194/egusphere-2026-6962
Preprint. Discussion started: 20 November 2026
© Author(s) 2026. CC BY 4.0 License.

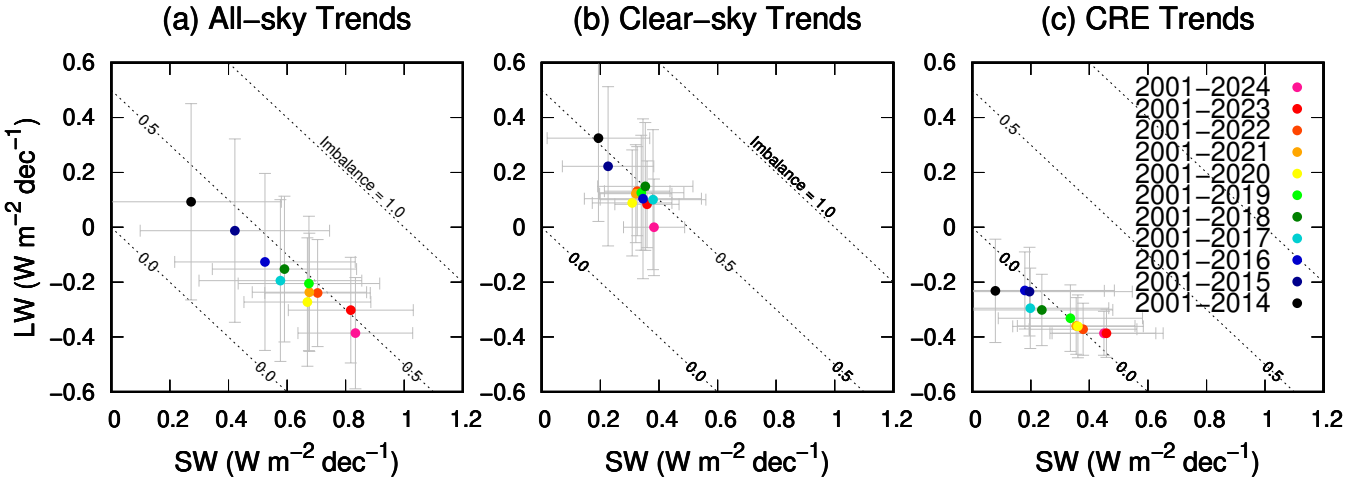


Figure 2. CERES satellite-retrieved radiative-flux trends. Trends for (**a**) all-sky, (**b**) clear-sky, and (**c**) CRE. Each panel shows trends calculated over analysis periods from 2001–2014, extending the trend window by one year to 2001–2024 (cumulative trend analysis). Dashed contours indicate the imbalance of net trends. Error bars represent 95% confidence intervals for the estimated global-mean linear trend.

More specifically, for CRE trends, the positive trend is dominated by SW (+0.45 $\mathrm{W\,m^{-2}\,dec^{-1}}$) particularly over tropical ocean, North Pacific, and North Atlantic (Figure 1g), largely contributing to the all-sky SW distribution (Figure 1a). The positive SW CRE trend coincides with decreases in cloud coverage and cloud optical thickness (Figures S2a and S2b), consistent with recent reports based on multiple satellite retrievals and reanalysis (Goessling et al., 2024; Salzen et al., 2025). The positive SW CRE trend is largely but not completely offset by a negative LW CRE trend (-0.39 $\mathrm{W\,m^{-2}\,dec^{-1}}$), yielding a small positive net CRE trend (+0.06 $\mathrm{W\,m^{-2}\,dec^{-1}}$). The spatial distribution mirrors the SW pattern with the sign reversed (Figure 1h). This pattern is qualitatively consistent with decreased cloud coverage and the associated increase in LW emission to space and may also reflect a shift toward lower, warmer radiatively effective cloud levels (Figures S2c, S2d, and S3), particularly over the central Pacific, off California, and the western coast of North Africa (20°N–40°N). The resulting net CRE trend is therefore small but positive, although its geographical pattern strongly influences the all-sky net EEI trend together with the clear-sky net trend (Figures 1c, 1f, and 1i).

The above results are based on the 2001–2024 trend, and it is important to note that EEI trends have changed year by year (Figure 2). The all-sky net EEI trend increases from +0.37 $\mathrm{W\,m^{-2}\,dec^{-1}}$ for 2001–2014 to +0.45 $\mathrm{W\,m^{-2}\,dec^{-1}}$ for 2001–2024 (Figure 2a). The shift in the EEI trend is modest but persistent as the analysis period is extended, consistent with a sustained component superimposed on internal variability. This variability, including ENSO and decadal sea surface temperature (SST)-pattern changes, can modulate CRE and Earth's energy budget (Zhou et al., 2016), although recent attribution studies suggest that internal variability alone is unlikely to explain the observed TOA radiative trends (Raghuraman et al., 2023; Yukimoto et al., 2026). Despite the modest change in the net EEI trend, the SW and LW components change substantially. Extending

https://doi.org/10.5194/egusphere-2026-6962
Preprint. Discussion started: 20 November 2026
© Author(s) 2026. CC BY 4.0 License.

the analysis period from 2001–2014 to 2001–2024 increases the positive SW radiative-flux trend from +0.27 $\mathrm{W\,m^{-2}\,dec^{-1}}$ to +0.83 $\mathrm{W\,m^{-2}\,dec^{-1}}$, while the LW trend reverses sign from +0.09 $\mathrm{W\,m^{-2}\,dec^{-1}}$ to -0.39 $\mathrm{W\,m^{-2}\,dec^{-1}}$.

Over the past decade, the increase in the all-sky net EEI is attributed to a larger strengthening of the positive SW trend than the smaller weakening of the negative LW trend; the former is dominated by CRE contributions, whereas the latter is dominated by clear-sky contributions (Figures 2b and 2c). Nevertheless, clear-sky and CRE contributions remain of comparable importance (Raghuraman et al., 2021). EEI trends are strongly influenced by both aerosols and clouds in response to recent anthropogenic changes and resulting warming (Chen et al., 2024; Hakuba et al., 2024). Therefore, accurate climate predictions require better simulation of EEI trends for all-sky, clear-sky, and CRE conditions to match observational fingerprints.

3.2 Linkage between radiative-flux trends and ECS

Because EEI trends are observable quantities linked to future warming, constraining the unknown ECS parameter through the fundamental relationship between EEI, ERF, and global temperature records would be highly valuable (Michibata et al., 2025). However, when plotting the all-sky net EEI trends against ECS values using the CMIP6 models, almost no correlation is found (Figure 3a), consistent with a recent study (Myhre et al., 2025). This lack of correlation arises from several confounding factors between EEI trends and ECS, including 1) uncertainties in ERF, particularly aerosol-cloud interactions (Bellouin et al., 2020; Stier et al., 2024), 2) ocean heat-uptake efficiency and efficacy (Gregory et al., 2024), and 3) time-varying feedbacks, often referred to as the "pattern effect" associated with SST (Andrews et al., 2022; Armour et al., 2024) and the spatial dependence of aerosol forcing (Williams et al., 2022).

Interestingly, a robust correlation between EEI trends and ECS emerges when the net EEI trend is decomposed into SW and LW components, which holds for both all-sky (Figures 3a–3c) and clear-sky (Figures 3d–3f) conditions. For SW, a positive correlation is observed because increased SW absorption contributes to greater warming. Recent aerosol reductions contribute to this relationship (Hodnebrog et al., 2024; Samset et al., 2025) under clear-sky conditions (Figure 3e), and cloud dissipation can also enhance SW absorption. Additional analyses show coherent cloud reductions over the past two decades (Figures 4 and S2a, and Table S2). The satellite-retrieved decrease in cloud coverage (-0.11 $\mathrm{\%\,dec^{-1}}$, statistically significant at the 95% confidence level) is consistent with ERA5 reanalysis (Goessling et al., 2024). The cloud-coverage trend shows a moderate correlation with the EEI trend (Figures 4 and 5) and hence may play a key role in further constraining ECS (discussed later). For LW, a negative correlation is simulated, with higher-ECS models tending to show more negative LW radiative-flux trends. This relationship likely reflects intermodel differences in transient warming and the associated LW radiative response, both of which are influenced by ocean heat uptake and adjustment timescales. Thus, although the correlation has a plausible physical interpretation, it should not be interpreted as reflecting ECS alone.

An additional advantage of decomposing the EEI trend, particularly for clear-sky conditions, is its narrower trend uncertainty relative to CRE (Figure S4). Despite known challenges in clear-sky retrieval (Loeb et al., 2021b), this trend is the most stable and thus has a narrower uncertainty range in the clear-sky EEI (Loeb et al., 2024). This contributes to a tighter constraint on the modeled radiative-flux trends and ECS (Figures 3e and 3f). The CMIP6 models simulate the clear-sky SW flux trend well, indicating that ECS values above 4.5 K fall outside the uncertainty range of CERES retrievals. In contrast, the clear-sky LW

https://doi.org/10.5194/egusphere-2026-6962
Preprint. Discussion started: 20 November 2026
© Author(s) 2026. CC BY 4.0 License.

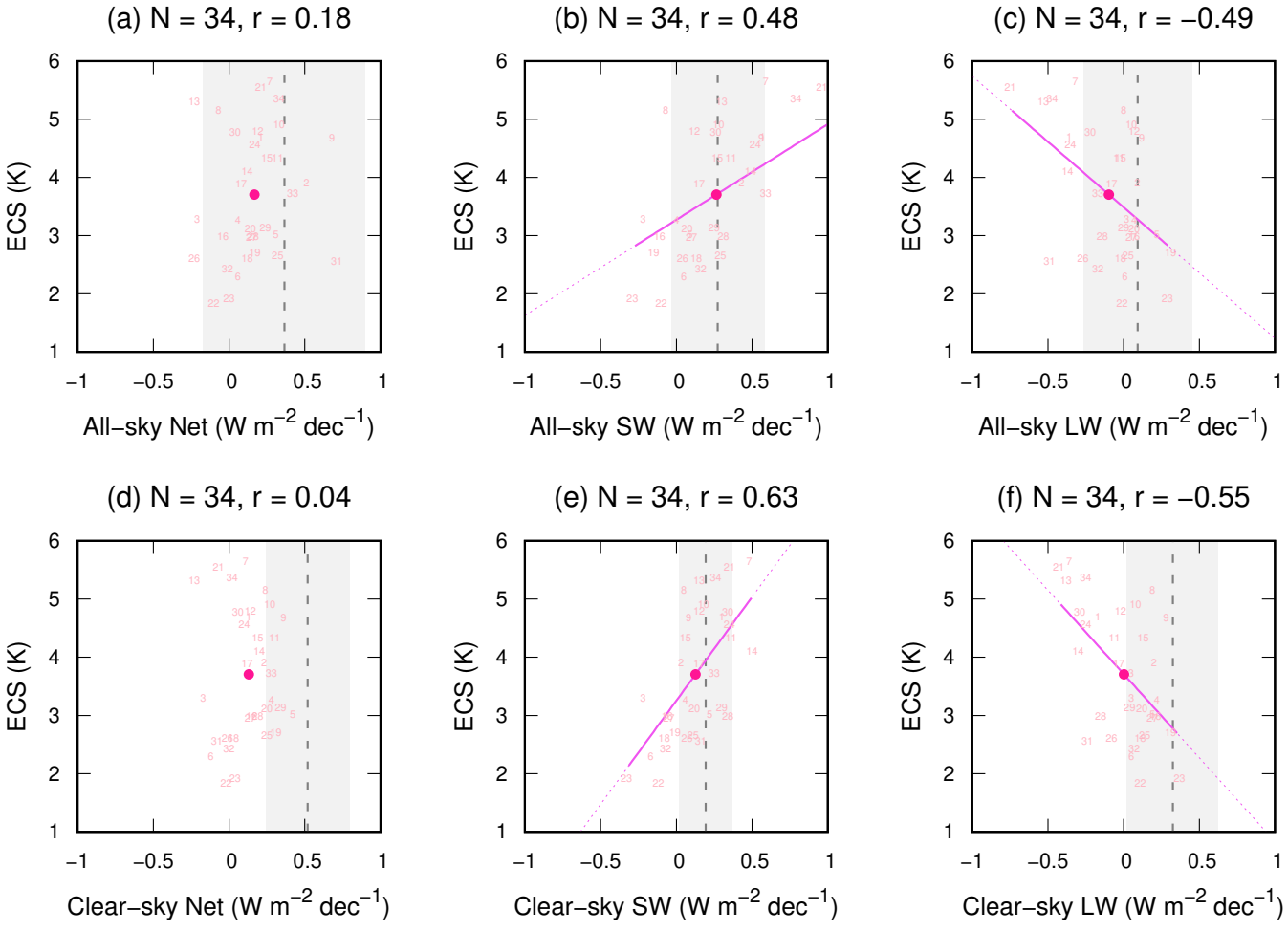


Figure 3. Relationship between ECS and radiative-flux trends. (**a**) all-sky net EEI, (**b**) all-sky SW, (**c**) all-sky LW, (**d**) clear-sky net, (**e**) clear-sky SW, and (**f**) clear-sky LW trends for CMIP6 models. Numbers correspond to models summarized in Table S1, and the circle indicates the multimodel mean. Linear regression lines are shown for the SW and LW components, with dashed segments indicating the extrapolated portions. Dashed black lines with grey shading show the CERES satellite estimate with a 95% confidence interval. The correlation coefficient between the radiative-flux trend and ECS (r) is shown in each panel.

trend is underestimated by most of the analyzed models. This emergent constraint from the clear-sky LW trend appears to support lower-ECS models (Figure 3f) with at least a multimodel mean ($< \sim$3.5 K), which aligns with constraints based on recent temperature trends (Tokarska et al., 2020; Modak and Mauritsen, 2021; Olonscheck and Rugenstein, 2024; Skeie et al., 2024). However, when the CERES retrieval uncertainty is considered, ECS values below 2.0 K are also excluded.

https://doi.org/10.5194/egusphere-2026-6962
Preprint. Discussion started: 20 November 2026
© Author(s) 2026. CC BY 4.0 License.

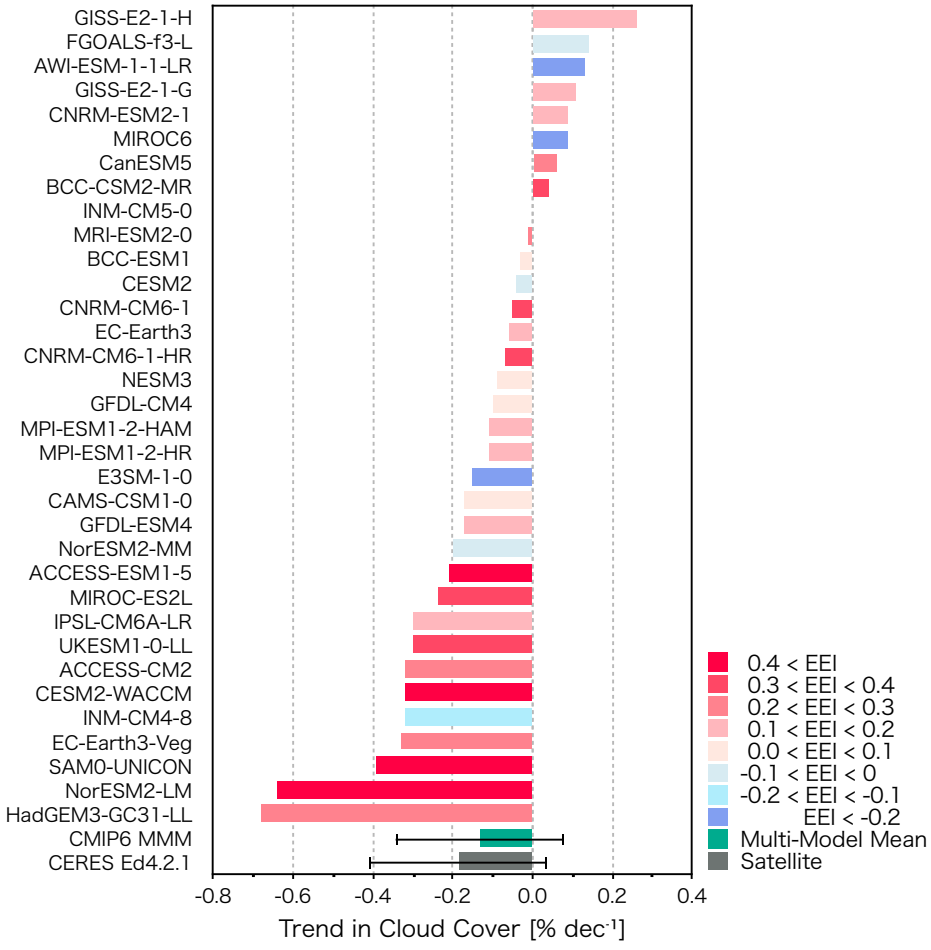


Figure 4. Trends in cloud cover ($\%\,\mathrm{dec}^{-1}$) for 34 CMIP6 models (blue to red) and CERES satellite retrievals (grey) for the trend period 2001-2014. Model colors indicate all-sky net EEI trends, and green shows the CMIP6 multimodel mean.

3.3 Compensating errors in CMIP6 radiative-flux trends

Several recent studies have rejected lower-ECS models (Chenal et al., 2022; Myhre et al., 2025). Nevertheless, it is premature to conclude that our results are inconsistent with them, because a physically plausible multimodel relationship does not necessarily hold in the real world. Although this cannot be fully verified, examining how CMIP6 models capture the satellite-retrieved radiative-flux trends across different scenes and components is a straightforward and essential step toward understanding sources of model uncertainty (Stephens et al., 2022; Schmidt et al., 2023; Myhre et al., 2025).

Here we compare the nine radiative-flux trends between CERES satellite retrievals and 34 CMIP6 models (Figure 6). The CMIP6 models reproduce the CERES-retrieved all-sky EEI trend within the uncertainty range, and the multimodel mean

https://doi.org/10.5194/egusphere-2026-6962
Preprint. Discussion started: 20 November 2026
© Author(s) 2026. CC BY 4.0 License.

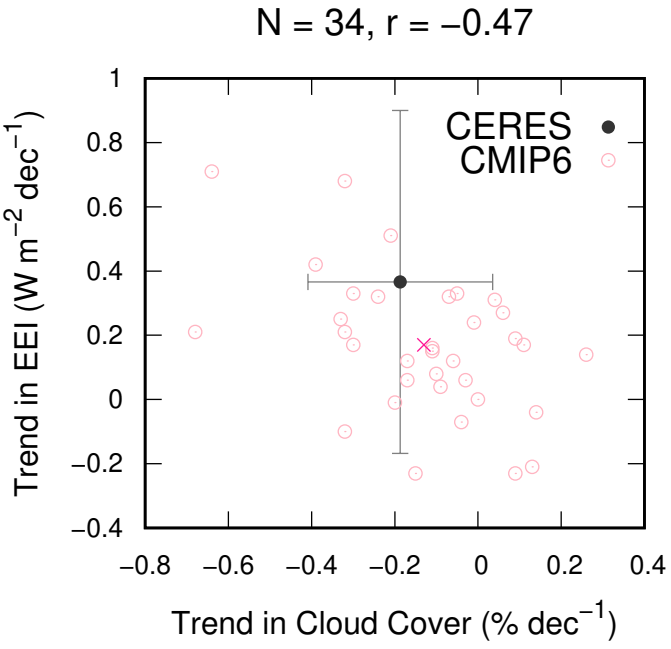


Figure 5. Relationship between cloud cover trends and all-sky net EEI trends for the period 2001-2014. The correlation coefficient between the two (r) among 34 CMIP6 models is also shown, and the multimodel mean is indicated by a cross mark. Error bars represent the trend uncertainties in the CERES satellite at the 95% confidence interval.

roughly captures it, particularly for the SW component, despite slightly underestimating the all-sky LW trends. However, they misrepresent clear-sky and CRE trends with biases that compensate for each other.

More specifically, the CMIP6 models substantially underestimated the net clear-sky trend (+0.13 $\mathrm{W\,m^{-2}\,dec^{-1}}$) against CERES retrieval (+0.52 $\mathrm{W\,m^{-2}\,dec^{-1}}$), which exceeds the top of the ensemble range. Given that historical simulations of surface temperature are roughly consistent with observations (Forster et al., 2021), this lower LW trend is likely associated with biases in the horizontal pattern of surface warming (Andrews et al., 2022) and/or in the vertical warming structure (Mitchell et al., 2020). These biases may in turn be linked to biased water-vapor trends (Allan et al., 2022). Examining the causes of the large discrepancies in the clear-sky LW trend merits further investigation but is beyond the scope of this study. Nevertheless, the clear-sky SW trend shows better agreement between CERES and CMIP6 multimodel ensembles, implying that the models capture recent aerosol-induced forcing and surface-albedo changes, although multimodel diversity remains large.

For CRE, the CERES-retrieved negative net CRE trend (-0.15 $\mathrm{W\,m^{-2}\,dec^{-1}}$) is not captured in the CMIP6 multimodel mean (+0.04 $\mathrm{W\,m^{-2}\,dec^{-1}}$). The bias originates primarily from the LW CRE trend rather than from the SW CRE trend. Because the negative LW CRE trend dominates over the tropics, particularly in convective regions (Figure 1h) that show a decreased cloud trend (Figure S2a), the model bias in the LW CRE trend may be attributable to incomplete anvil thinning (Raghuraman et al., 2024; Sokol et al., 2024) due to coarser vertical model resolution (Bony et al., 2016; McKim et al., 2024) and/or incomplete responses of tropical deep convection to climate warming (Hirota et al., 2022; Stephens et al., 2024). Although this requires

https://doi.org/10.5194/egusphere-2026-6962
Preprint. Discussion started: 20 November 2026
© Author(s) 2026. CC BY 4.0 License.

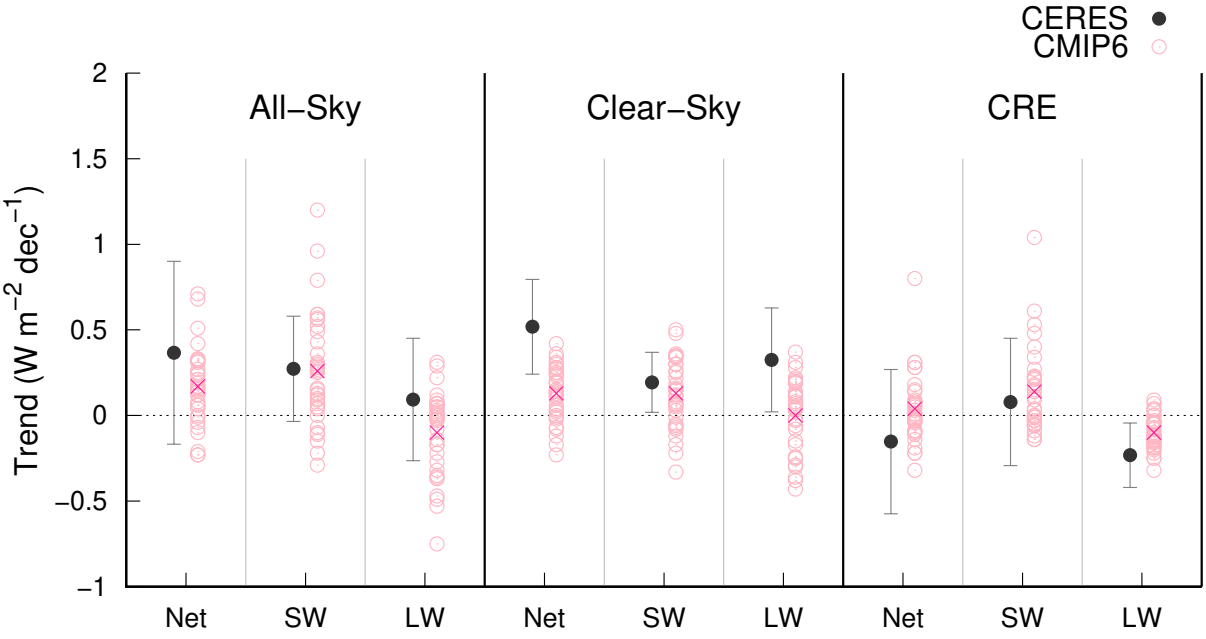


Figure 6. Radiative-flux trends for net, SW, and LW radiation under all-sky, clear-sky, and CRE. CERES observations are shown in black, with error bars indicating 95% uncertainty on the linear regression. Results from 34 CMIP6 models are plotted as red circles, and the multimodel mean is shown with a cross. Trends are calculated over the period 2001-2014 for both CERES and CMIP6 models to match the overlapping historical simulation period.

further investigations, the finding that biases primarily originate from the LW component rather than the SW component for both clear-sky and CRE is notable, as many EEI studies have focused on enhanced SW absorption associated with declining aerosol emissions and cloud dissipation.

In conclusion, compensating biases between clear-sky and CRE trends complicate the physical interpretation of emergent relationship among EEI, ERF, and feedbacks, and ECS. EEI-based emergent constraints on ECS remain potentially useful, but their robustness requires consistency between models and observations across SW, LW, clear-sky, and CRE components (Figures 3 and 6).

4 Discussion and conclusions

This study showed that decomposed radiative-flux trends (SW and LW, clear-sky and CRE) provide useful constraints on ECS and can help physically elucidate the sources of model–observation discrepancies. Correlations between SW and LW trends and ECS are stronger than those between net trends and ECS across CMIP6 models, particularly under clear-sky conditions. Considering the trend uncertainty in CERES satellite retrievals, the multimodel relationships yield an estimated ECS range of 2.0–4.5 K. This inferred range is based on the 2001–2014 period and probably depends on the analysis period because CERES

https://doi.org/10.5194/egusphere-2026-6962
Preprint. Discussion started: 20 November 2026
© Author(s) 2026. CC BY 4.0 License.

radiative-flux trends vary over time (Figure 2). This time dependence is attributable to the combined effects of radiative forcing, feedback responses, and internal variability, including pattern effects (Zhou et al., 2016; Andrews et al., 2022; Armour et al., 2024). Therefore, the ECS range should be regarded as an indicative constraint rather than a definitive estimate of ECS.

An important caveat is that apparent agreement in the all-sky net EEI trend does not necessarily ensure agreement in the component trends. Although CMIP6 models broadly reproduce the all-sky net EEI trend within observational uncertainty, biases in clear-sky and CRE trends compensate for each other (Figure 6). To understand the mechanisms underlying these biases, the combined use of cloud cover trends provides a useful approach because cloud cover is an observable metric independent of energy trends. Cloud cover trends covary with EEI trends, largely in association with SW CRE, and some CMIP6 models even misrepresent the sign relative to the negative trend observed (Figures 4 and 5). Recent studies have also suggested that reductions in low-cloud coverage and associated cloud reflectance have contributed substantially to the observed SW and EEI trends, thereby providing an observational fingerprint of cloud feedback and aerosol-cloud interactions (Ceppi et al., 2026b; Zelinka et al., 2026). Although the present study used total cloud coverage, trends in different cloud types and vertical structures should also be investigated in future studies, together with decomposed radiative-flux trends and feedback components (Voigt et al., 2024; Wall et al., 2025; Wilson Kemsley et al., 2025).

A further limitation arises from natural variability. The multimodel-mean spatial patterns of the nine TOA radiative-flux trends (Figure S5) are broadly similar to those from CERES observations. This similarity suggests a consistent forced contribution shared across models and observations because internally generated variability that is independent across models is reduced in the multimodel mean. Nevertheless, CERES observations represent a single realization of the climate record, whereas internal climate variability is partially averaged out within the multimodel ensemble (Fyfe et al., 2016). Thus, we cannot ignore contributions from internal variability, including SST pattern changes (Zhou et al., 2016; Andrews et al., 2022; Armour et al., 2024), which may affect the magnitude and components of the observed trends, particularly over short periods. Biases in aerosol emission scenarios can also introduce uncertainty into the trends simulated by models (Lund et al., 2023; Park and Soden, 2025), thereby motivating long-term simulations with updated forcing datasets under the CERESMIP protocol (Schmidt et al., 2023) and in upcoming CMIP7 models (Ceppi et al., 2026a).

Overall, our results suggest that the all-sky net EEI trend alone is insufficient for evaluating the physical mechanisms underlying simulated historical evolution. Assessing the simulated trends in different radiative-flux components together with the associated cloud cover trend provides more process-oriented information on how models physically represent climate change in a manner consistent with observations (Myhre et al., 2025; Bimpiri et al., 2026). This approach remains potentially useful for constraining ECS and feedbacks, but compensating errors across components, observational uncertainties, and sensitivity to the selected analysis period and scenario dependence should be carefully considered.

Without consistency between models and observations in the current climate, trend-based inferences for past and future climates may remain confounded by structural model errors.

https://doi.org/10.5194/egusphere-2026-6962
Preprint. Discussion started: 20 November 2026
© Author(s) 2026. CC BY 4.0 License.

Data availability. The CERES EBAF Edition 4.2.1 dataset is available at https://doi.org/10.5067/TERRA-AQUA-NOAA20/CERES/EBAF_L3B004.2.1 (Doelling, 2026). The CMIP6 datasets are publicly available at https://esgf-node.llnl.gov/search/cmip6/.

Author contributions. TM conceptualized the study, performed the formal analysis, and wrote the original manuscript. MN provided guidance on the analysis and contributed to manuscript revisions.

Competing interests. The authors declare there are no conflicts of interest.

Acknowledgements. This research was supported by the JST FOREST Program (Grant JPMJFR206Y); the Japan Society for the Promotion of Science KAKENHI (Grants JP25K07404, JP26H02569, and JP26K03071); the Environment Research and Technology Development Fund (Grants JPMEERF21S12004 and JPMEERF20262RA2) of the Environmental Restoration and Conservation Agency, provided by the Ministry of Environment of Japan; and the Advanced Studies of Climate Change Projection (SENTAN) of the Ministry of Education, Culture, Sports, Science, and Technology (Grant JPMXD0722680395). Numerical simulations were performed using the SX-Aurora TSUBASA supercomputer system at the National Institute for Environmental Studies, Japan.

https://doi.org/10.5194/egusphere-2026-6962
Preprint. Discussion started: 20 November 2026
© Author(s) 2026. CC BY 4.0 License.

References

Allan, R. P. and Merchant, C. J.: Reconciling Earth's growing energy imbalance with ocean warming, Environmental Research Letters, 20, https://doi.org/10.1088/1748-9326/adb448, 2025.

Allan, R. P., Willett, K. M., John, V. O., and Trent, T.: Global Changes in Water Vapor 1979–2020, Journal of Geophysical Research: Atmospheres, 127, e2022JD036 728, https://doi.org/10.1029/2022JD036728, 2022.

Andrews, T., Bodas-Salcedo, A., Gregory, J. M., Dong, Y., Armour, K. C., Paynter, D., Lin, P., Modak, A., Mauritsen, T., Cole, J. N., Medeiros, B., Benedict, J. J., Douville, H., Roehrig, R., Koshiro, T., Kawai, H., Ogura, T., Dufresne, J. L., Allan, R. P., and Liu, C.: On the Effect of Historical SST Patterns on Radiative Feedback, Journal of Geophysical Research: Atmospheres, 127, https://doi.org/10.1029/2022JD036675, 2022.

Armour, K. C., Proistosescu, C., Dong, Y., Hahn, L. C., Blanchard-Wrigglesworth, E., Pauling, A. G., Jnglin Wills, R. C., Andrews, T., Stuecker, M. F., Po-Chedley, S., Mitevski, I., Forster, P. M., and Gregory, J. M.: Sea-surface temperature pattern effects have slowed global warming and biased warming-based constraints on climate sensitivity, Proceedings of the National Academy of Sciences of the United States of America, 121, 1–11, https://doi.org/10.1073/pnas.2312093121, 2024.

Bellouin, N., Quaas, J., Gryspeerdt, E., Kinne, S., Stier, P., Watson-Parris, D., Boucher, O., Carslaw, K., Christensen, M., Daniau, A., Dufresne, J., Feingold, G., Fiedler, S., Forster, P., Gettelman, A., Haywood, J., Lohmann, U., Malavelle, F., Mauritsen, T., McCoy, D., Myhre, G., Mülmenstädt, J., Neubauer, D., Possner, A., Rugenstein, M., Sato, Y., Schulz, M., Schwartz, S., Sourdeval, O., Storelvmo, T., Toll, V., Winker, D., and Stevens, B.: Bounding global aerosol radiative forcing of climate change, Reviews of Geophysics, 58, e2019RG000 660, https://doi.org/10.1029/2019rg000660, 2020.

Bimpiri, K., Hocking, T., and Mauritsen, T.: Climate models with moderate climate sensitivity best simulate the magnitude of Earth's energy imbalance, Earth System Dynamics, 17, 877–892, https://doi.org/10.5194/esd-17-877-2026, 2026.

Bony, S., Stevens, B., Coppin, D., Becker, T., Reed, K. A., Voigt, A., and Medeiros, B.: Thermodynamic control of anvil cloud amount, Proceedings of the National Academy of Sciences of the United States of America, 113, 8927–8932, https://doi.org/10.1073/pnas.1601472113, 2016.

Ceppi, P., Bodas-Salcedo, A., Zelinka, M. D., Andrews, T., Brient, F., Chadwick, R., Dai, A.-Z., Gregory, J. M., Hwang, Y.-T., Kang, S. M., Kay, J. E., Mauritsen, T., Ogura, T., Tselioudis, G., Watanabe, M., Webb, M. J., and Wing, A. A.: The Cloud Feedback Model Intercomparison Project (CFMIP) contribution to CMIP7, Geoscientific Model Development, 19, 8693–8708, https://doi.org/10.5194/gmd-19-8693-2026, 2026a.

Ceppi, P., Wilson Kemsley, S., Andersen, H., Andrews, T., Kramer, R. J., Nowack, P., Wall, C. J., and Zelinka, M. D.: Emerging low-cloud feedback and adjustment in global satellite observations, Atmospheric Chemistry and Physics, 26, 4153–4171, https://doi.org/10.5194/acp-26-4153-2026, 2026b.

Cesana, G. V., Ackerman, A. S., Fridlind, A. M., Silber, I., Genio, A. D. D., Zelinka, M. D., Chepfer, H., Khadir, T., and Roehrig, R.: Observational constraint on a feedback from supercooled clouds reduces projected warming uncertainty, Communications Earth and Environment, 5, 181, https://doi.org/10.1038/s43247-024-01339-1, 2024.

Chen, Y., Haywood, J., Wang, Y., Malavelle, F., Jordan, G., Peace, A., Partridge, D. G., Cho, N., Oreopoulos, L., Grosvenor, D., Field, P., Allan, R. P., and Lohmann, U.: Substantial cooling effect from aerosol-induced increase in tropical marine cloud cover, Nature Geoscience, 17, 404–410, https://doi.org/10.1038/s41561-024-01427-z, 2024.

https://doi.org/10.5194/egusphere-2026-6962
Preprint. Discussion started: 20 November 2026
© Author(s) 2026. CC BY 4.0 License.



Chenal, J., Meyssignac, B., Ribes, A., and Guillaume-Caste, R.: Observational Constraint on the Climate Sensitivity to Atmospheric CO2 Concentrations Changes Derived from the 1971-2017 Global Energy Budget, Journal of Climate, 35, 4469–4483, https://doi.org/10.1175/JCLI-D-21-0565.1, 2022.

Cheng, L., von Schuckmann, K., Minière, A., Hakuba, M. Z., Purkey, S., Schmidt, G. A., and Pan, Y.: Ocean heat content in 2023, Nature Reviews Earth & Environment, 5, 232–234, https://doi.org/10.1038/s43017-024-00539-9, 2024.

Doelling, D.: CERES Energy Balanced and Filled (EBAF) TOA Monthly means data in netCDF Edition4.2.1, https://doi.org/10.5067/TERRA-AQUA-NOAA20/CERES/EBAF-TOA_L3B004.2.1, dataset, 2026.

Forster, P. M., Storelvmo, T., Armour, K., W. Collins, Dufresne, J., Frame, D., D. J. Lunt, Mauritsen, T., Palmer, M. D., Watanabe, M., Wild, M., and Zhang, H.: The Earth's Energy Budget, Climate Feedbacks, and Climate Sensitivity, IPCC AR6, Chapter 7, pp. 923–1054, https://doi.org/10.1017/9781009157896.009.923, 2021.

Forster, P. M., Smith, C., Walsh, T., Lamb, W. F., Lamboll, R., Hall, B., Hauser, M., Ribes, A., Rosen, D., Gillett, N. P., Palmer, M. D., Rogelj, J., Von Schuckmann, K., Trewin, B., Allen, M., Andrew, R., Betts, R. A., Borger, A., Boyer, T., Broersma, J. A., Buontempo, C., Burgess, S., Cagnazzo, C., Cheng, L., Friedlingstein, P., Gettelman, A., Gütschow, J., Ishii, M., Jenkins, S., Lan, X., Morice, C., Mühle, J., Kadow, C., Kennedy, J., Killick, R. E., Krummel, P. B., Minx, J. C., Myhre, G., Naik, V., Peters, G. P., Pirani, A., Pongratz, J., Schleussner, C. F., Seneviratne, S. I., Szopa, S., Thorne, P., Kovilakam, M. V., Majamäki, E., Jalkanen, J. P., Van Marle, M., Hoesly, R. M., Rohde, R., Schumacher, D., Van Der Werf, G., Vose, R., Zickfeld, K., Zhang, X., Masson-Delmotte, V., and Zhai, P.: Indicators of Global Climate Change 2023: annual update of key indicators of the state of the climate system and human influence, Earth System Science Data, 16, 2625–2658, https://doi.org/10.5194/essd-16-2625-2024, 2024.

Fyfe, J. C., Meehl, G. A., England, M. H., Mann, M. E., Santer, B. D., Flato, G. M., Hawkins, E., Gillett, N. P., Xie, S. P., Kosaka, Y., and Swart, N. C.: Making sense of the early-2000s warming slowdown, Nature Climate Change, 6, 224–228, https://doi.org/10.1038/nclimate2938, 2016.

Gettelman, A., Christensen, M. W., Diamond, M. S., Gryspeerdt, E., Manshausen, P., Stier, P., Watson-Parris, D., Yang, M., Yoshioka, M., and Yuan, T.: Has Reducing Ship Emissions Brought Forward Global Warming?, Geophysical Research Letters, 51, e2024GL109 077, https://doi.org/10.1029/2024GL109077, 2024.

Goessling, H. F., Rackow, T., and Jung, T.: Recent global temperature surge intensified by record-low planetary albedo, Science, 7280, 1–11, https://doi.org/10.1126/science.adq7280, 2024.

Gregory, J. M., Bloch-Johnson, J., Couldrey, M. P., Exarchou, E., Griffies, S. M., Kuhlbrodt, T., Newsom, E., Saenko, O. A., Suzuki, T., Wu, Q., Urakawa, S., and Zanna, L.: A new conceptual model of global ocean heat uptake, Climate Dynamics, 62, 1669–1713, https://doi.org/10.1007/s00382-023-06989-z, 2024.

Hakuba, M. Z., Fourest, S., Boyer, T., and Meyssignac, B.: Trends and Variability in Earth's Energy Imbalance and Ocean Heat Uptake Since 2005, Surveys in Geophysics, https://doi.org/10.1007/s10712-024-09849-5, 2024.

Hansen, J., Sato, M., and Kharecha, P.: Earth's energy imbalance and implications, Atmospheric Chemistry and Physicshe, 11, 13 421–13 449, https://doi.org/10.5194/acp-11-13421-2011, 2011.

Hirota, N., Michibata, T., Shiogama, H., Ogura, T., and Suzuki, K.: Impacts of Precipitation Modeling on Cloud Feedback in MIROC6, Geophysical Research Letters, 49, e2021GL096 523, https://doi.org/10.1029/2021gl096523, 2022.

Hodnebrog, Ø., Myhre, G., Jouan, C., Andrews, T., Forster, P. M., Jia, H., Loeb, N. G., Olivié, D. J. L., Paynter, D., Quaas, J., Raghuraman, S. P., and Schulz, M.: Recent reductions in aerosol emissions have increased Earth's energy imbalance, Communications Earth and Environment, 5, 1–9, https://doi.org/10.1038/s43247-024-01324-8, 2024.

https://doi.org/10.5194/egusphere-2026-6962
Preprint. Discussion started: 20 November 2026
© Author(s) 2026. CC BY 4.0 License.

Kato, S., Rose, F. G., Rutan, D. A., Thorsen, T. J., Loeb, N. G., Doelling, D. R., Huang, X., Smith, W. L., Su, W., and Ham, S. H.: Surface irradiances of edition 4.0 Clouds and the Earth's Radiant Energy System (CERES) Energy Balanced and Filled (EBAF) data product, Journal of Climate, 31, 4501–4527, https://doi.org/10.1175/JCLI-D-17-0523.1, 2018.

Loeb, N. G., Doelling, D., Wang, H., Su, W., Nguyen, C., Corbett, J., Liang, L., Mitrescu, C., Rose, F., and Kato, S.: Surface irradiances of edition 4.0 Clouds and the Earth's Radiant Energy System (CERES) Energy Balanced and Filled (EBAF) data product, Journal of Climate, 31, 4501–4527, https://doi.org/10.1175/JCLI-D-17-0523.1, 2018.

Loeb, N. G., Johnson, G. C., Thorsen, T. J., Lyman, J. M., Rose, F. G., and Kato, S.: Satellite and Ocean Data Reveal Marked Increase in Earth's Heating Rate, Geophysical Research Letters, 48, e2021GL093 047, https://doi.org/10.1029/2021GL093047, 2021a.

Loeb, N. G., Su, W., Bellouin, N., and Ming, Y.: Changes in Clear-Sky Shortwave Aerosol Direct Radiative Effects Since 2002, Journal of Geophysical Research: Atmospheres, 126, https://doi.org/10.1029/2020JD034090, 2021b.

Loeb, N. G., Mayer, M., Kato, S., Fasullo, J. T., Zuo, H., Senan, R., Lyman, J. M., Johnson, G. C., and Balmaseda, M.: Evaluating Twenty-Year Trends in Earth's Energy Flows from Observations and Reanalyses, Journal of Geophysical Research: Atmospheres, 127, e2022JD036 686, https://doi.org/10.1029/2022jd036686, 2022.

Loeb, N. G., Ham, S. H., Allan, R. P., Thorsen, T. J., Meyssignac, B., Kato, S., Johnson, G. C., and Lyman, J. M.: Observational Assessment of Changes in Earth's Energy Imbalance Since 2000, Surveys in Geophysics, 45, 1757–1783, https://doi.org/10.1007/s10712-024-09838-8, 2024.

Loeb, N. G., Thorsen, T. J., Kato, S., Rose, F. G., Hodnebrog, Ø., and Myhre, G.: Emerging hemispheric asymmetry of Earth's radiation, Proceedings of the National Academy of Sciences, 122, e2511595 122, https://doi.org/10.1073/pnas.2511595122, 2025.

Lund, M. T., Myhre, G., Skeie, R. B., Samset, B. H., and Klimont, Z.: Implications of differences between recent anthropogenic aerosol emission inventories for diagnosed AOD and radiative forcing from 1990 to 2019, Atmospheric Chemistry and Physics, 23, 6647–6662, https://doi.org/10.5194/acp-23-6647-2023, 2023.

Lutsko, N. J., Luongo, M. T., Wall, C. J., and Myers, T. A.: Correlation Between Cloud Adjustments and Cloud Feedbacks Responsible for Larger Range of Climate Sensitivities in CMIP6, Journal of Geophysical Research: Atmospheres, 127, e2022JD037 486, https://doi.org/10.1029/2022JD037486, 2022.

Mauritsen, T., Tsushima, Y., Meyssignac, B., Loeb, N. G., Hakuba, M., Pilewskie, P., Cole, J., Suzuki, K., Ackerman, T. P., Allan, R. P., Andrews, T., Bender, F. A., Bloch-Johnson, J., Bodas-Salcedo, A., Brookshaw, A., Ceppi, P., Clerbaux, N., Dessler, A. E., Donohoe, A., Dufresne, J. L., Eyring, V., Findell, K. L., Gettelman, A., Gristey, J. J., Hawkins, E., Heimbach, P., Hewitt, H. T., Jeevanjee, N., Jones, C., Kang, S. M., Kato, S., Kay, J. E., Klein, S. A., Knutti, R., Kramer, R., Lee, J. Y., McCoy, D. T., Medeiros, B., Megner, L., Modak, A., Ogura, T., Palmer, M. D., Paynter, D., Quaas, J., Ramanathan, V., Ringer, M., von Schuckmann, K., Sherwood, S., Stevens, B., Tan, I., Tselioudis, G., Sutton, R., Voigt, A., Watanabe, M., Webb, M. J., Wild, M., and Zelinka, M. D.: Earth's Energy Imbalance More Than Doubled in Recent Decades, AGU Advances, 6, e2024AV001 636, https://doi.org/10.1029/2024AV001636, 2025.

McCoy, D. T., Field, P., Bodas-Salcedo, A., Elsaesser, G. S., and Zelinka, M. D.: A Regime-Oriented Approach to Observationally Constraining Extratropical Shortwave Cloud Feedbacks, Journal of Climate, 33, 9967–9983, https://doi.org/10.1175/jcli-d-19-0987.1, 2020.

McKim, B., Bony, S., and Dufresne, J. L.: Weak anvil cloud area feedback suggested by physical and observational constraints, Nature Geoscience, 17, 392–397, https://doi.org/10.1038/s41561-024-01414-4, 2024.

Meehl, G. A., Senior, C. A., Eyring, V., Flato, G., Lamarque, J.-F., Stouffer, R. J., Taylor, K. E., and Schlund, M.: Context for interpreting equilibrium climate sensitivity and transient climate response from the CMIP6 Earth system models, Science Advances, 6, eaba1981, https://doi.org/10.1126/sciadv.aba1981, 2020.

https://doi.org/10.5194/egusphere-2026-6962
Preprint. Discussion started: 20 November 2026
© Author(s) 2026. CC BY 4.0 License.

Michibata, T., Wall, C. J., Hirota, N., Duran, B. M., and Nozawa, T.: Recent Advances in the Observation and Modeling of Aerosol-Cloud Interactions, Cloud Feedbacks, and Earth's Energy Imbalance: A Review, Current Pollution Reports, 11, 50, https://doi.org/10.1007/s40726-025-00382-6, 2025.

Mitchell, D. M., Eunice Lo, Y. T., Seviour, W. J., Haimberger, L., and Polvani, L. M.: The vertical profile of recent tropical temperature trends: Persistent model biases in the context of internal variability, Environmental Research Letters, 15, https://doi.org/10.1088/1748-9326/ab9af7, 2020.

Modak, A. and Mauritsen, T.: The 2000–2012 Global Warming Hiatus More Likely With a Low Climate Sensitivity, Geophysical Research Letters, 48, e2020GL091 779, https://doi.org/10.1029/2020GL091779, 2021.

Myhre, G., Hodnebrog, Ø., Loeb, N., and Forster, P. M.: Observed trend in Earth energy imbalance may provide a constraint for low climate sensitivity models, Science, pp. 1210–1213, https://doi.org/10.1126/science.adt0647, 2025.

Nakanishi, M. and Michibata, T.: How does cloud emissivity feedback affect present and future Arctic warming?, Ocean-Land-Atmosphere Research, 4, 0089, https://doi.org/10.34133/olar.0089, 2025.

Olonscheck, D. and Rugenstein, M.: Coupled Climate Models Systematically Underestimate Radiation Response to Surface Warming, Geophysical Research Letters, 51, e2023GL106 909, https://doi.org/10.1029/2023GL106909, 2024.

Park, C. and Soden, B. J.: Negligible contribution from aerosols to recent trends in Earth's energy imbalance, Science Advances, 11, eadv9429, https://doi.org/10.1126/sciadv.adv9429, 2025.

Raghuraman, S. P., Paynter, D., and Ramaswamy, V.: Anthropogenic forcing and response yield observed positive trend in Earth's energy imbalance, Nature Communications, 12, 1–10, https://doi.org/10.1038/s41467-021-24544-4, 2021.

Raghuraman, S. P., Paynter, D., Menzel, R., and Ramaswamy, V.: Forcing, Cloud Feedbacks, Cloud Masking, and Internal Variability in the Cloud Radiative Effect Satellite Record, Journal of Climate, 36, 4151–4167, https://doi.org/10.1175/JCLI-D-22-0555.1, 2023.

Raghuraman, S. P., Medeiros, B., and Gettelman, A.: Observational Quantification of Tropical High Cloud Changes and Feedbacks, Journal of Geophysical Research: Atmospheres, 129, https://doi.org/10.1029/2023JD039364, 2024.

Salzen, K. V., Akingunola, A., Cole, J. N. S., Digby, R. A. R., Doherty, S. J., Fraser-leach, L., Gryspeerdt, E., Sigmond, M., and Wood, R.: Reduced aerosol pollution diminished cloud reflectivity over the North Atlantic and Northeast Pacific, Nature Communications, 16, 9433, https://doi.org/10.1038/s41467-025-65127-x, 2025.

Samset, B., Wilcox, L., Allen, R., Stjern, C., Lund, M., Ahmadi, S., Elling, M., Fraser-Leach, L., Griffiths, P., Keeble, J., Koshiro, T., Kushner, P., Lewinschal, A., Makkonen, R., Merikanto, J., Nabat, P., Narazenko, L., O'Donnell, D., Oshima, N., Rumbold, S., Takemura, T., Tsigaridis, K., and Westervelt, D.: China's aerosol cleanup has contributed strongly to the recent acceleration in global warming, Communications Earth and Environment, 6, 543, https://doi.org/10.1038/s43247-025-02527-3, 2025.

Schmidt, G. A., Andrews, T., Bauer, S. E., Durack, P. J., Loeb, N. G., Ramaswamy, V., Arnold, N. P., Bosilovich, M. G., Cole, J., Horowitz, L. W., Johnson, G. C., Lyman, J. M., Medeiros, B., Michibata, T., Olonscheck, D., Paynter, D., Raghuraman, S. P., Schulz, M., Takasuka, D., Tallapragada, V., Taylor, P. C., and Ziehn, T.: CERESMIP: A climate modeling protocol to investigate recent trends in the Earth's Energy Imbalance, Frontiers in Climate, 5, 1202 161, https://doi.org/10.3389/fclim.2023.1202161, 2023.

Sherwood, S., Webb, M. J., Annan, J. D., Armour, K. C., Forster, P. M., Hargreaves, J. C., Hegerl, G., Klein, S. A., Marvel, K. D., Rohling, E. J., Watanabe, M., Andrews, T., Braconnot, P., Bretherton, C. S., Foster, G. L., Hausfather, Z., von der Heydt, A. S., Knutti, R., Mauritsen, T., Norris, J. R., Proistosescu, C., Rugenstein, M., Schmidt, G. A., Tokarska, K. B., and Zelinka, M. D.: An assessment of Earth's climate sensitivity using multiple lines of evidence, Reviews of Geophysics, 58, e2019RG000 678, https://doi.org/10.1029/2019rg000678, 2020.

https://doi.org/10.5194/egusphere-2026-6962
Preprint. Discussion started: 20 November 2026
© Author(s) 2026. CC BY 4.0 License.

Skeie, R. B., Myhre, G., Aldrin, M., Holden, M., Bang Husebye, R., and Storelvmo, T.: The aerosol radiative forcing pathway crucial for observational constrained climate sensitivity, Earth System Dynamics, 15, 1435–1458, 2024.

Sokol, A. B., Wall, C. J., and Hartmann, D. L.: Greater climate sensitivity implied by anvil cloud thinning, Nature Geoscience, 17, 398–403, https://doi.org/10.1038/s41561-024-01420-6, 2024.

Stephens, G. L., Hakuba, M. Z., Kato, S., Gettleman, A., Dufresne, J. L., Andrews, T., Cole, J. N., Willem, U., and Mauritsen, T.: The changing nature of Earth's reflected sunlight, Proceedings of the Royal Society A: Mathematical, Physical and Engineering Sciences, 478, https://doi.org/10.1098/rspa.2022.0053, 2022.

Stephens, G. L., Shiro, K. A., Hakuba, M. Z., Takahashi, H., Pilewskie, J. A., Andrews, T., Stubenrauch, C. J., and Wu, L.: Tropical Deep Convection, Cloud Feedbacks and Climate Sensitivity, Surveys in Geophysics, 45, 1903–1931, https://doi.org/10.1007/s10712-024-09831-1, 2024.

Stier, P., van den Heever, S. C., Christensen, M. W., Gryspeerdt, E., Dagan, G., Saleeby, S. M., Bollasina, M., Donner, L., Emanuel, K., Ekman, A. M. L., Feingold, G., Field, P., Forster, P. M., Haywood, J., Kahn, R., Koren, I., Kummerow, C., L'Ecuyer, T., Lohmann, U., Ming, Y., Myhre, G., Quaas, J., Rosenfeld, D., Samset, B., Seifert, A., Stephens, G., and Tao, W.-K.: Multifaceted aerosol effects on precipitation, Nature Geoscience, 17, 719–732, https://doi.org/10.1038/s41561-024-01482-6, 2024.

Tan, I. and Storelvmo, T.: Evidence of Strong Contributions From Mixed-Phase Clouds to Arctic Climate Change, Geophysical Research Letters, 46, 2894–2902, https://doi.org/10.1029/2018GL081871, 2019.

Taylor, K. E., Crucifix, M., Braconnot, P., Hewitt, C. D., Doutriaux, C., Broccoli, A. J., Mitchell, J. F., and Webb, M. J.: Estimating shortwave radiative forcing and response in climate models, Journal of Climate, 20, 2530–2543, https://doi.org/10.1175/JCLI4143.1, 2007.

Tokarska, K. B., Stolpe, M. B., Sippel, S., Fischer, E. M., Smith, C. J., Lehner, F., and Knutti, R.: Past warming trend constrains future warming in CMIP6 models, Science Advances, 6, 1–13, https://doi.org/10.1126/sciadv.aaz9549, 2020.

Trenberth, K. E., Fasullo, J. T., and Balmaseda, M. A.: Earth's energy imbalance, Journal of Climate, 27, 3129–3144, https://doi.org/10.1175/JCLI-D-13-00294.1, 2014.

Trepte, Q. Z., Bedka, K. M., Chee, T. L., Minnis, P., Sun-Mack, S., Yost, C. R., Chen, Y., Jin, Z., Hong, G., Chang, F. L., and Smith, W. L.: Global Cloud Detection for CERES Edition 4 Using Terra and Aqua MODIS Data, IEEE Transactions on Geoscience and Remote Sensing, 57, 9410–9449, https://doi.org/10.1109/TGRS.2019.2926620, 2019.

Voigt, A., North, S., Gasparini, B., and Ham, S. H.: Atmospheric cloud-radiative heating in CMIP6 and observations and its response to surface warming, Atmospheric Chemistry and Physics, 24, 9749–9775, https://doi.org/10.5194/acp-24-9749-2024, 2024.

Von Schuckmann, K., Minière, A., Gues, F., Cuesta-Valero, F. J., Kirchengast, G., Adusumilli, S., Straneo, F., Ablain, M., Allan, R. P., Barker, P. M., Beltrami, H., Blazquez, A., Boyer, T., Cheng, L., Church, J., Desbruyeres, D., Dolman, H., Domingues, C. M., García-García, A., Giglio, D., Gilson, J. E., Gorfer, M., Haimberger, L., Hakuba, M. Z., Hendricks, S., Hosoda, S., Johnson, G. C., Killick, R., King, B., Kolodziejczyk, N., Korosov, A., Krinner, G., Kuusela, M., Landerer, F. W., Langer, M., Lavergne, T., Lawrence, I., Li, Y., Lyman, J., Marti, F., Marzeion, B., Mayer, M., MacDougall, A. H., McDougall, T., Monselesan, D. P., Nitzbon, J., Otosaka, I., Peng, J., Purkey, S., Roemmich, D., Sato, K., Sato, K., Savita, A., Schweiger, A., Shepherd, A., Seneviratne, S. I., Simons, L., Slater, D. A., Slater, T., Steiner, A. K., Suga, T., Szekely, T., Thiery, W., Timmermans, M. L., Vanderkelen, I., Wjiffels, S. E., Wu, T., and Zemp, M.: Heat stored in the Earth system 1960-2020: where does the energy go?, Earth System Science Data, 15, 1675–1709, https://doi.org/10.5194/essd-15-1675-2023, 2023.

https://doi.org/10.5194/egusphere-2026-6962
Preprint. Discussion started: 20 November 2026
© Author(s) 2026. CC BY 4.0 License.



Wall, C. J., Paynter, D., Qin, Y., Debolskiy, M., Duffy, M. L., Michibata, T., Duran, B. M., Lutsko, N. J., Ma, P.-L., Medeiros, B., Storelvmo, T., and Zhao, M.: Decomposing Cloud Radiative Feedbacks by Cloud-Top Phase, Journal of Climate, 38, 4023–4043, https://doi.org/10.1175/jcli-d-24-0538.1, 2025.

Williams, A. I., Stier, P., Dagan, G., and Watson-Parris, D.: Strong control of effective radiative forcing by the spatial pattern of absorbing aerosol, Nature Climate Change, 12, 735–742, https://doi.org/10.1038/s41558-022-01415-4, 2022.

Wilson Kemsley, S., Nowack, P., and Ceppi, P.: Climate Models Underestimate Global Decreases in High-Cloud Amount With Warming, Geophysical Research Letters, 52, e2024GL113 316, https://doi.org/10.1029/2024GL113316, 2025.

Yukimoto, S., Kawai, H., Oshima, N., and Deushi, M.: Emerging Effective Radiative Forcing in the Radiative Imbalance since 2010 Key Points :, Geophysical Research Letters, 53, e2025GL119 913, https://doi.org/10.1029/2025GL119913, 2026.

Zelinka, M. D., Myers, T. A., McCoy, D. T., Po-Chedley, S., Caldwell, P. M., Ceppi, P., Klein, S. A., and Taylor, K. E.: Causes of Higher Climate Sensitivity in CMIP6 Models, Geophysical Research Letters, 47, e2019GL085 782, https://doi.org/10.1029/2019GL085782, 2020.

Zelinka, M. D., Myers, T. A., Qin, Y., Chao, L.-W., Klein, S. A., Po-Chedley, S., Ma, P.-L., Wall, C. J., Ceppi, P., and Gettelman, A.: Recent cloud trends and extremes reaffirm established bounds on cloud feedback and aerosol-cloud interactions, Communications Earth and Environment, 7, 615, https://doi.org/10.1038/s43247-026-03461-8, 2026.

Zhou, C., Zelinka, M. D., and Klein, S. A.: Impact of decadal cloud variations on the Earth's energy budget, Nature Geoscience, 9, 871–874, https://doi.org/10.1038/ngeo2828, 2016.